

https://doi.org/10.21608/zumj.2025.419825.4147

Volume 31, Issue 11 November. 2025

Manuscript ID:ZUMJ-2509-4147 DOI:10.21608/zumj.2025.419825.4147

**ORIGINAL ARTICLE** 

# Using a Quantitative Assessment Tool in Diffusion Weighted Magnetic Resonance Imaging in Patients with Non-Neoplastic Vertebrogenic Low Back Pain

Ahmed Awad Bessar, Khaled Mohamed Shawky, Mai Nabil Mohamed Attia\*, Rania Mostafa Abd El Rahman Hassan

Radio-diagnosis department, Faculty of Medicine, Zagazig University, Zagazig, Egypt.

## \*Corresponding author:

Mai Nabil Mohamed Attia

#### **Email:**

nmai07318@gmail.com

Submit Date: 02-09-2025 Revise Date: 23-09-2025 Accept Date: 02-10-2025

#### **ABSTRACT**

**Background:** The addition of apparent diffusion coefficient (ADC) measurements and diffusion-weighted imaging (DWI) can address the limitations of conventional MRI by offering complementary quantitative and qualitative diffusion markers. We aimed to evaluate the diagnostic utility of added ADC values and DWI relative to standard MRI, particularly for distinguishing Modic type I changes from early spondylodiscitis, while also improving the characterization of various non-neoplastic lumbar vertebral lesions.

**Methods:** In this case–control study, 48 patients with vertebrogenic low back pain and 48 controls underwent lumbar MRI, including DWI at a b-value of 800 s/mm². In 25 patients with indeterminate conventional findings (hypointense on T1WI and hyperintense on T2WI), additional DWI acquisitions at b = 50 and 500 s/mm² were performed to compare with b = 800 s/mm². ADC values were measured using regions of interest, and qualitative DWI signs (claw sign, amorphous increased signal) were assessed.

**Results:** Within cases, Modic I changes (37.5%) were most frequent, followed by benign fractures and early infectious endplate changes (14.6% each). Mean ADC was significantly higher in cases (1.10  $\pm$  0.47  $\times 10^{-3}$  mm²/s) than controls (0.26  $\pm$  0.08, p < 0.001). Among subgroups, benign fractures and Modic II changes had the highest ADC values, while Modic III showed the lowest. At b = 800 s/mm², DWI achieved a sensitivity of 85.7%, a specificity of 94.4%, and an accuracy of 92%. ADC cutoff >1.19  $\times 10^{-3}$  mm²/s provided 100% specificity but lower sensitivity (79.2%). The claw sign achieved perfect diagnostic accuracy, while amorphous increased signal also performed strongly (accuracy 96%).

**Conclusions:** ADC measurements and DWI substantially improve the characterization of various benign lumbar vertebral lesions, outperforming conventional MRI alone. The combination of quantitative ADC thresholds with qualitative diffusion signs offers a reliable, non-invasive diagnostic approach that enhances clinical confidence and supports better patient management.

**Keywords:** Diffusion Weighted; Magnetic Resonance Imaging; Non-Neoplastic; Vertebrogenic Low Back Pain.

#### INTRODUCTION

Low back pain (LBP) remains the leading cause of long-term disability worldwide, particularly among working-age

adults. The global burden continues to rise with population aging and ongoing exposure to physical and psychosocial risk factors. It is projected that the number of individuals

Bessar, et al 5362 | Page

affected will increase further by 2050. Despite this burden, the precise etiologies of LBP are often multifactorial and incompletely understood [1].

Among spinal tissues, intervertebral disc degeneration, characterized by biochemical disruption. depletion. structural metabolic alteration, frequently coexists with pathological changes in the vertebral endplates and adjacent bone marrow. These endplate lesions, known as Modic changes (MCs), have been implicated as potential generators. inflammatory pain An environment, mediated by cytokines and immune cells, may spread from disrupted discs into subchondral bone, leading to marrow edema and nociceptive stimulation

Recent meta-analyses report that MCs are present in around 35% of lumbar spines, with advanced age, disc degeneration, endplate damage, and certain biomechanical risk factors increasing their likelihood [4]. Cross-sectional data further suggest that Type I and larger-extent MCs are associated with more intense pain, greater disability, and reduced quality of life [5].

To address vertebrogenic sources of LBP more specifically, the clinical entity of vertebrogenic pain has been refined. Patients with vertebrogenic pain typically present with non-radiating axial lumbar pain (often L3–S1), worsened by flexion, sitting, or prolonged load, and with comparatively limited radicular features. Basivertebral nerve (BVN) innervation of vertebral provides plausible endplates a pathophysiologic basis, and BVN ablation has emerged as a minimally invasive treatment showing promising results in both randomized and real-world studies [6].

While conventional MRI (T1 and T2-weighted sequences) remains foundational for assessing structural degeneration, its qualitative readings are limited by the high prevalence of degenerative findings in

asymptomatic individuals. obscuring attribution of symptoms to specific lesions [7]. Modic classification helps standardize reporting, but differentiation between early Modic changes. infection. and other overlapping etiologies often remains challenging [8].

Emerging imaging modalities such as diffusion-weighted imaging (DWI) offer microstructural contrast by assessing water diffusivity, membrane integrity, extracellular space, and cellularity. These techniques may enhance lesion characterization beyond morphology alone, degenerative distinguishing endplate changes infection better from and correlating imaging findings with clinical phenotypes [3,8].

Despite these advances, quantitative thresholds (e.g., ADC values), optimal imaging parameters (e.g., b-values), and definitions for clinically meaningful changes remain inconsistent [7]. Accordingly, this study aimed to investigate the role of advanced MRI in identifying endplate changes in patients with non-neoplastic vertebrogenic low back pain and to compare its diagnostic accuracy with conventional imaging.

#### **METHODS**

#### Study design and population

This case-control study was carried out at the Radiodiagnosis Department of our institute, over 6 months (January–June 2025). Forty-eight patients with lumbar vertebral abnormalities and 48 age- and sexmatched controls with normal lumbar MRIs were included.

Approval was obtained from our university's Institutional Review Board (IRB# 11178-8/10-2023). Written informed consent was obtained from all participants. The study followed the principles of the Declaration of Helsinki.

The study included adult patients above 18 years old who underwent lumbar spine MRI.

**Bessar**, et al **5363** | P a g e

Eligible participants were those presenting with clinically significant low back pain, as well as individuals diagnosed with acute spinal fractures localized between the L1 and S1 vertebral levels. In addition, patients with confirmed spinal infections within the same lumbar region (L1–S1) were also considered for inclusion.

Exclusion criteria included patients with isolated radicular leg pain without low back pain, neoplastic causes, prior lumbar spine surgery, or contraindications to MRI, such as pacemakers, defibrillators, pacing wires, vascular or cerebral clips, cochlear or other magnet-containing implants. Also excluded were those with vertebral pathology outside L1–S1, bedbound status or neurological impairment affecting mobility or follow-up, ongoing extended-release opioid therapy, body mass index >40, or suboptimal image quality due to motion artifacts or poor signal-to-noise ratio.

#### Clinical evaluation

All patients underwent a comprehensive clinical assessment, including demographics, symptom duration, medical history, and prior imaging. **Functional** disability was quantified using the Western Ontario and McMaster Universities Arthritis (WOMAC) questionnaire. Index validated tool comprises 24 items across three subscales: Pain (5 items), Stiffness (2 items), and Physical Function (17 items). Each item was scored on a Likert scale (0-4), producing subscale totals (Pain: 0-20, Stiffness: 0-8, Function: 0-68). Higher reflected disability. scores greater Administration requires ~12 minutes per patient (**Fig.2S**) [9].

#### **Imaging protocol**

All examinations were performed on a 1.5-Tesla MRI scanner (Philips Medical Systems). Standard protocols included sagittal and axial T1- and T2-weighted sequences.

Sagittal STIR was performed in selected patients with indeterminate findings or suspected marrow edema (in 32 cases). It was not performed for all cases because of longer acquisition time, lower signal-to-noise ratio, and limited added value when conventional sequences were already conclusive. Contrast-enhanced T1-weighted sequences were obtained when clinically indicated (in 8 cases).

Sagittal images were acquired with a 4-mm section thickness, 380-mm field of view, 258 x 512 matrix, and the following sequences: T1-weighted spin echo (SE) (600/12 [repetition time TR msec/echo time TE msec]) and T2-weighted SE (5000/120 TR/TE), Axial images were acquired with 4-mm section thickness, 380-mm field of view, 192 x 256 matrix, and the following sequences: T1-weighted SE (750/15 TR/TE) and T2-weighted SE (5500/120 TR/TE).

Diffusion-weighted imaging (DWI) corresponding apparent diffusion coefficient (ADC) maps was performed in all cases and controls. A sagittal echo-planar DWI sequence was obtained using a b-value of 800 s/mm<sup>2</sup> across all subjects. In a subgroup with indeterminate patients conventional findings (hypointense on T1WI and hyperintense on T2WI), additional DWI acquisitions at b = 50 and 500 s/mm<sup>2</sup> were performed to compare with b = 800 s/mm<sup>2</sup>, based on evidence supporting enhanced with higher lesion detection diffusion gradients [10].

The average acquisition time for DWI was approximately 2 minutes. Regions of interest were manually placed on sagittal ADC maps to encompass the largest lesion area, with ADC values automatically generated in mm²/s. Qualitative assessment of lesion signal intensity was also conducted, using adjacent disc, fat, and muscle as reference tissues on T1- and T2-weighted images.

DWI was performed with a maximum b-value of 800 s/mm<sup>2</sup>, as higher b-values in

**Bessar**, et al **5364** | P a g e

spinal imaging can lead to signal-to-noise loss and increased susceptibility artifacts, particularly in echo-planar sequences, which reduce image reliability. Previous studies on spinal infection and Modic changes recommend a maximum b-value of 800 s/mm² to balance diffusion sensitivity and image quality [11].

#### **Reference Standard**

Infectious spondylitis was diagnosed based on a combination of clinical data, laboratory tests (elevated ESR, CRP, leukocytosis, or positive blood cultures), imaging follow-up & post-contrast study in some cases. Degenerative Modic type I changes were confirmed in patients with no clinical or laboratory evidence of infection and stable/improving symptoms on follow-up. All patients were clinically radiologically monitored for at least 6 months. For other cases with benign lesions, diagnosis was confirmed by clinical data and CT studies.

#### Statistical analysis:

Statistical analysis was performed using SPSS version 26 (IBM Corp., Armonk, NY, USA). Continuous data were expressed as mean ± SD and compared using the independent t-test, while categorical variables were analyzed with the Chi-square or Fisher's exact test. Diagnostic accuracy of DWI/ADC was assessed against clinical and laboratory follow-up, with sensitivity, specificity, predictive values, and accuracy derived from 2×2 tables. Receiver operating (ROC) curves determined characteristic optimal ADC cutoffs for differentiating Modic type I changes from infection, with AUC values reported. Significance was set at p < 0.05.

#### **RESULTS**

The average age of the studied case group was  $(52.8\pm11.3)$  years, ranging from 22-75 years. while the average age of the control group was  $(49.9\pm11.5)$  years, ranging from 21-70 years. No significant differences

were revealed in age (p=0.22), sex distribution (p=0.41), or weight (p=0.25) between cases and controls. Associated symptoms also showed significant variation (MCp=0.023), particularly with higher rates of LL paresthesia (22.9%) in controls and LL pain and inability to move (each 6.3%) exclusively in the cases group (**Table 1**). The mean duration of vertebrogenic LBP was  $1.47 \pm 1.12$  years, and the mean WOMAC score for the case group was  $58.52 \pm 18.47$ , with scores ranging from 30 to 93.

Table 2 summarizes ADC values across spinal pathologies. The overall mean ADC in the cases group was significantly higher  $(1.10 \pm 0.47 \times 10^{-3} \text{ mm}^2/\text{sec})$  than in the  $(0.26 \pm 0.08;$ p < 0.001). group Among cases, benign fractures exhibited the highest ADC  $(1.79 \pm 0.25)$ , followed by  $(1.46 \pm 0.45)$ Modic  $\Pi$ and typical hemangiomas  $(1.35 \pm 0.34)$ , while the lowest were values observed in Modic Ш  $(0.55 \pm 0.05)$ .

**Table 3** presents MRI-based final diagnoses across groups. In the cases group, the most frequent findings were Modic I changes (37.5%),benign fractures and infectious endplate changes (each 14.6%), and hemangiomas (12.5%). In contrast, the control group predominantly exhibited disc bulge/herniation (39.6%),back muscle spasm (33.3%), and normal lumbar MRI (27.1%).

The b-value of 800 s/mm² demonstrates the highest diagnostic performance, with a sensitivity of 85.7%, a specificity of 94.4%, and an overall accuracy of 92%. In contrast, lower b-values (50 and 500 s/mm²) show limited specificity and accuracy, indicating their suboptimal utility in differential diagnosis (**Table 4**).

Conventional MRI had an overall accuracy of 84.8%, but lower specificity (77.8%), while ADC values (using a threshold of  $>1.19\times10^{-3}$  mm<sup>2</sup>/s) showed sensitivity

Bessar, et al 5365 | Page

(79.2%), specificity (100%), NPV (64.3%) and PPV (100%), resulting in an overall accuracy of 82.1%. The amorphous increased signal showed high diagnostic performance, while the claw sign achieved perfect diagnostic performance (**Table 5**).

Table 1S outlines conventional MRI signal characteristics and associated findings. Among cases, 83.3% showed T1WI hypointensity and 89.6% showed T2WI hyperintensity in vertebral lesions. Loss of lumbar lordosis was the most common associated (62.5%),followed finding by disc bulge/herniation (37.5%). Controls exhibited a normal vertebral signal on MRI with facilitated diffusion on DWI.

Figure 1: A 68-year-old male presented with vertebrogenic low back pain of 8 months' duration. (A, B & C): Sagittal T1weighted MR image, sagittal T2-weighted MR image, sagittal STIR MR image of lumbar spine. Show (A) hypo-intensity, (B) hyperintensity signal, **(C)** hyperintensity signal at the involved bone marrow of both vertebral bodies at the (L2-3) level. (D, E & F): Sagittal diffusion-weighted MR image of lumbar spine with different b values: (D) b-value of 50 s/mm<sup>2</sup>, (E) b-value of 500 s/mm<sup>2</sup>, (F) b-value of 800 s/mm<sup>2</sup> showing amorphous increased hyperintensity signal at the involved bone marrow with increasing b-value. (G) a corresponding sagittal lumbar ADC map (to DWI at b value 800 s/mm<sup>2</sup>). The lesion showed restricted diffusion as indicated by a high signal at DWI and a low signal at ADC. The ROI on the lesion yields an ADC value of  $0.927 \times 10^{-3} \text{ mm}^2/\text{s}$ . This case was confirmed to have infective spondylodiscitis by laboratory findings (elevated ESR, CRP levels, and blood culture) and follow-up.

**Figure 2:** A 55-year-old male presented with vertebrogenic low back pain of 2 years duration. (A, B & C): Sagittal T1-weighted

MR image, sagittal T2WI, Sagittal STIR MR image of lumbar spine. Show (A) hypohyperintensity signal, (C) intensity. (B) hyperintensity signal at the involved bone marrow of both vertebral bodies at the (L2-3) level. (D, E& F): Sagittal diffusionweighted MR image of lumbar spine with different b values: (D) b-value of 50 s/mm<sup>2</sup>. (E) b-value of 500 s/mm<sup>2</sup>. (F) b-value of 800 s/mm<sup>2</sup>, the red arrows indicate the lesion at the vertebral endplate, demonstrating the claw sign across different sequences." The claw sign is a well-defined, curvilinear hyperintensity at the junction between normal and abnormal marrow signals in the vertebral endplates on DWI, "claw-like" forming a pattern that decreasing with increasing b-value. (G) sagittal lumbar DWI at b value 800 s/mm<sup>2</sup>&(H) corresponding sagittal lumbar The lesion shows restricted ADC map. diffusion (high signal at DWI, low at ADC map). The ROI on the lesion yields an ADC value of  $1.325 \times 10^{-3}$  mm<sup>2</sup>/s. This case was confirmed to have MODIC I degenerative changes by follow-up.

Figure 1S: A 30-year-old female presented with vertebrogenic low back pain (A, B, C, D &E). (A) Sagittal T1-weighted image of lumbar spine showing a hypointense lesion of the L2 vertebral body. (B) Sagittal T2weighted image of lumbar spine showing a hyperintense lesion of the L2 vertebral body. (C) Sagittal lumbar DWI at (b value 800 s/mm<sup>2</sup>): The vertebral body lesion shows an isointense signal. (D) Corresponding ADC map: The lesion shows a high signal, matching facilitated diffusion. ROI on the lesion (ADC value:  $1.823 \times 10^{-3} \text{ mm}^2/\text{sec}$ ). The case was confirmed to have an L2 compression fracture by CT (E). Sagittal lumbar spine CT shows a compression fracture of the L2 vertebrae.

**Bessar, et al 5366** | P a g e

**Table 1:** Baseline Demographic Data, Comorbidities, and Associated Symptoms Among Studied Groups (n=96)

Variable	Cases Group (n = 48)	Control Group (n = 48)	Test statistic	p-value
Age (years)				
Mean ± SD	52.8 ± 11.3	49.9 ± 11.5	t = 1.24	0.22
Range	22 – 75	21 – 70		
Sex (n, %)				
Male	20 (41.7%)	24 (50.0%)	$\chi^2 = 0.67$	0.41
Female	28 (58.3%)	24 (50.0%)		
Weight (kg)				
Mean ± SD	84.9 ± 12.4	$82.0 \pm 1.3$	t = 1.16	0.25
Range	64 – 120	60 –110		
Comorbidities (n, %)				
None	35 (72.9%)	42 (87.5%)		
DM	3 (6.3%)	3 (6.3%)		
HTN	3 (6.3%)	3 (6.3%)	$\chi^2 = 8.103*$	0.040*
HTN + DM	7 (14.6%)	0 (0.0%)		
Associated Symptoms				
( <b>n</b> , %)				
None	37 (77.1%)	32 (66.7%)		
LL Numbness	3 (6.3%)	5 (10.4%)		
LL Paresthesia	3 (6.3%)	11 (22.9%)	$\chi^2 = 9.628*$	MCp = 0.023*
LL Pain	2 (4.2%)	0 (0.0%)		
Inability to Move	3 (6.3%)	0 (0.0%)		

DM: Diabetes Mellitus; HTN: Hypertension; LL: Lower Limb; SD: Standard Deviation;  $\chi^2$ : Chi-square test; t: Independent t-test; MCp: Monte Carlo corrected p-value.  $p \le 0.05$  was considered statistically significant.

**Table 2:** Apparent Diffusion Coefficient (ADC) Values with various spinal pathologies among the Studied Groups

1		ADC ( $\times 10^{-3}$ mm <sup>2</sup> /sec)			
Final Diagnosis / Group	n	Mean ± SD	Range	Test statistic	p-value
Cases Subgroups					
Degenerative endplate	18	$1.29 \pm 0.07$	_	_	_
changes (Modic I)					
Early infectious endplate	7	$0.97 \pm 0.11$	_	=	_
changes					
Late infective	2	$0.80 \pm 0.01$	_	_	_
spondylodis citis					
Benign fractures	7	$1.79 \pm 0.25$	_	=	_
End plate changes (Modic II)	3	$1.46 \pm 0.45$	_	_	_
Facet joint osteoarthropathy	2	$0.85 \pm 0.07$	_	=	_
End plate changes (Modic III)	3	$0.55 \pm 0.05$	_	_	_
Hemangiomas (Atypical)	2	$0.80 \pm 0.57$	_	_	_
Hemangiomas (Typical)	4	$1.35 \pm 0.34$	_	_	_
Overall Cases Group	48	$1.10 \pm 0.47$	0.23 - 2.04		
Control Group	48	$0.26 \pm 0.08$	0.13 - 0.42	t = 10.1	<0.001*

ADC: Apparent Diffusion Coefficient; SD: Standard Deviation; t: Independent t-test.  $p \leq 0.05$  was considered statistically significant. \* Comparing Cases versus Control group using an independent t-test

Bessar, et al 5367 | Page

**Table 3:** MRI Final Diagnosis Among Studied Groups (n=96)

MRI Diagnosis	Cases Group (n = 48)	Control Group (n = 48)
End plate changes (Modic I)	18 (37.5%)	_
End plate changes (Modic II)	3 (6.3%)	_
End plate changes (Modic III)	3 (6.3%)	_
Early infectious endplate changes	7 (14.6%)	_
Infective spondylodiscitis	2 (4.2%)	_
Benign fractures	7 (14.6%)	_
Facet joint arthropathy	2 (4.2%)	_
Hemangiomas	6 (12.5%)	_
Disc bulge / Herniation	_	19 (39.6%)
Back muscle spasm	_	16 (33.3%)
Normal MRI lumbar spine	_	13 (27.1%)

MRI: Magnetic Resonance Imaging; Modic I/II/III: Types of vertebral endplate signal changes on MRI. All values are expressed as frequency (percentage).

**Table 4:** Agreement (sensitivity, specificity, and accuracy) for degenerative endplate changes (Modic I) and early infectious endplate (n = 25):

	Final Diagnosis			<b>S</b>	X			<b>x</b>	
	Modic	type 1	Infectious		Sensitivity	Specificity			Accuracy
	(n=18	3)	spondylitis		siti	cif	PPV	NPV	C C C
			$(\mathbf{n}=7)$		en	) jpe	PF	Z	Ac
	No.	%	No.	%	<b>3</b> 2	<b>S</b> 2			
b-value: 50smm <sup>-2</sup>									
Iso + Hypo	0	0.0	0	0.0	100.0	0.0	28.0	0	28.0
Hyperintense	18	100.0	7	100.0					
b-value: 500smm <sup>-2</sup>									
Iso + Hypo	2	11.1	0	0.0	100.0	11.1	30.4	100.0	36.0
Hyperintense	16	88.9	7	100.0					
b-value: 800smm <sup>-2</sup>									
Iso + Hypo	17	94.4	1	14.3	85.7	94.4	85.7	94.4	92.0
Hyperintense	1	5.6	6	85.7					

PPV: Positive predictive value NPV: Negative predictive value

**Table 5:** Diagnostic Accuracy in the Differentiation of Endplate Changes from Infectious Spondylitis

			PPV	NPV	Accuracy
Diagnostic Parameter	Sensitivity (%)	Specificity (%)	(%)	(%)	(%)
Conventional MRI	87.5	77.8	91.3	70.0	84.8
$ADC > 1.19 \times 10^{-3}$	79.2	100.0	100.0	64.3	82.1
mm²/sec					
Claw sign	100.0	100.0	100.0	100.0	100.0
Amorphous increased	96.4	95.8	96.1	95.7	96.0
signal					

MRI: Magnetic Resonance Imaging; ADC: Apparent Diffusion Coefficient; PPV: Positive Predictive Value; NPV: Negative Predictive Value.

Bessar, et al 5368 | Page

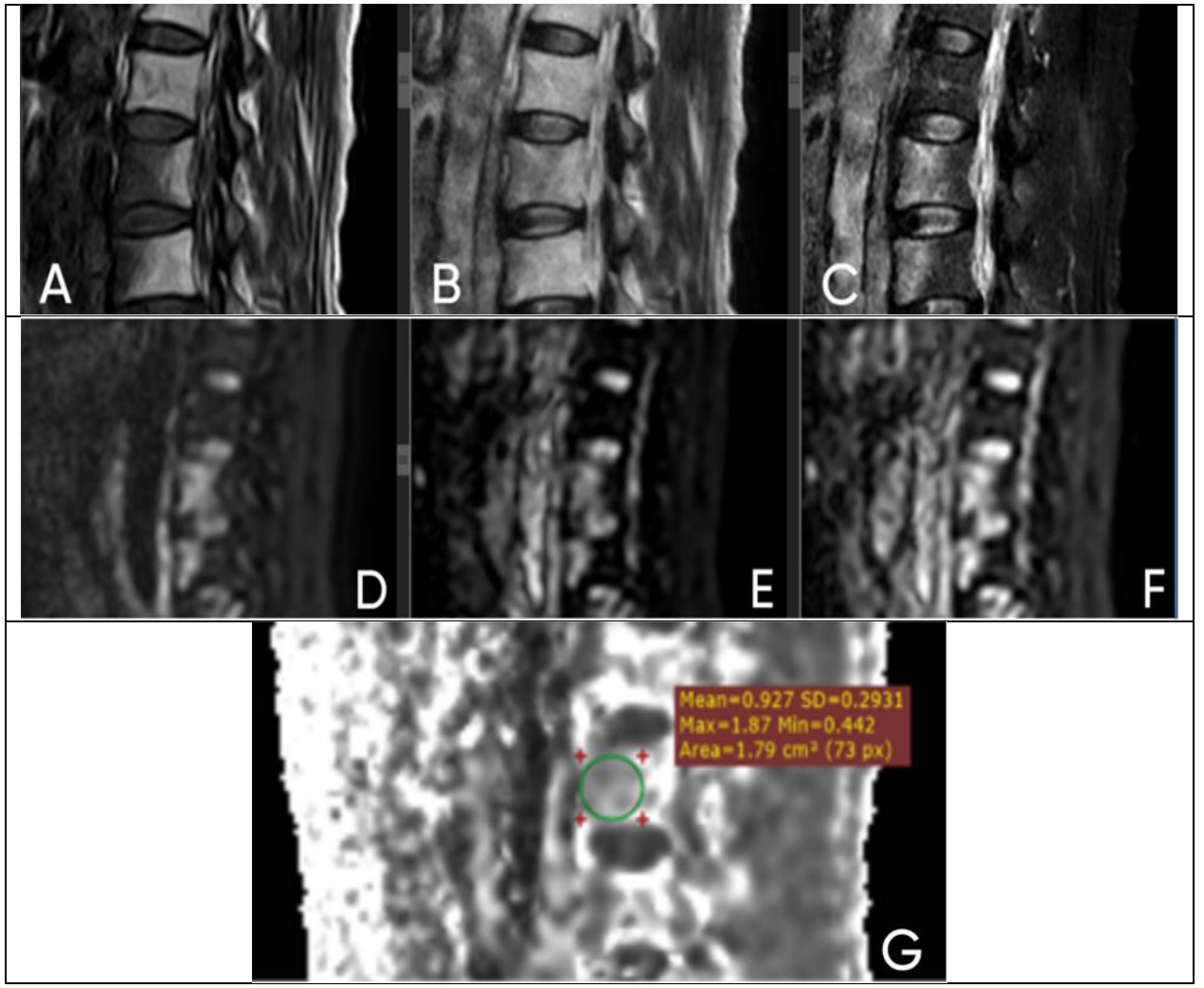
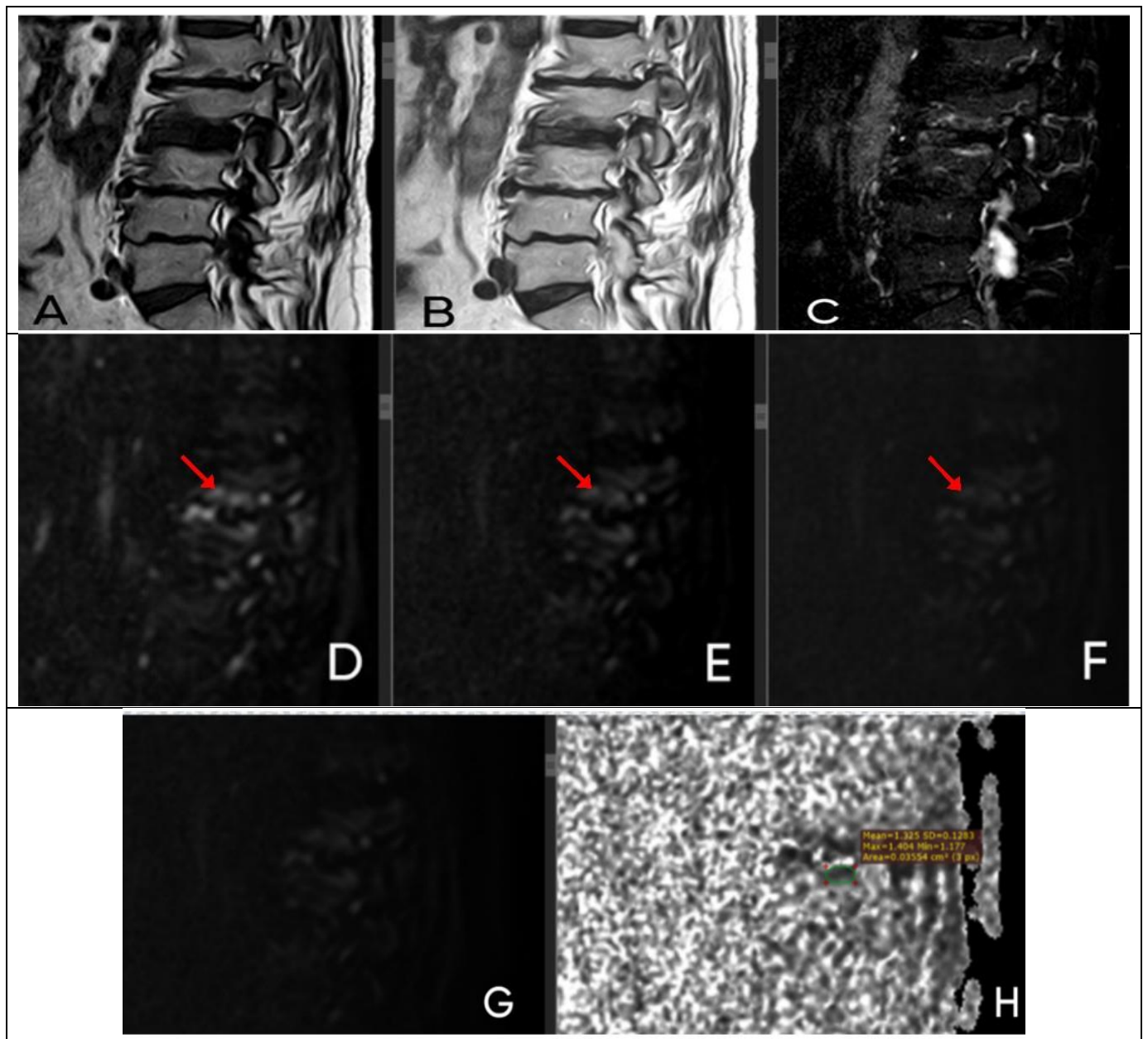


Figure 1: A 68-year-old male presented with vertebrogenic low back pain of 8 months' duration. (A, B & C): Sagittal T1weighted MR image, sagittal T2-weighted image, sagittal STIR MR image of lumbar Show hypo-intensity, spine. **(A)** signal, hyperintensity hyperintensity **(C)** signal at the involved bone marrow of both vertebral bodies at the (L2-3) level. (D, E & F): Sagittal diffusion-weighted MR image of lumbar spine with different b values: (D) b-value of 50 s/mm<sup>2</sup>, (E) b-value of 500 s/mm<sup>2</sup>, (F) b-value of 800 s/mm<sup>2</sup> showing

amorphous increased hyperintensity signal at the involved bone marrow with increasing b-value. (G) a corresponding sagittal lumbar ADC map (to DWI at b value 800 s/mm<sup>2</sup>). The lesion showed restricted diffusion as indicated by a high signal at DWI and a low signal at ADC. The ROI on the lesion yields an ADC value of  $0.927 \times 10^{-3} \text{ mm}^2/\text{s}$ . This case was confirmed to have infective spondylodiscitis laboratory findings by (elevated ESR, CRP levels, and blood culture) and follow-up.

**Bessar, et al 5369** | P a g e



**Figure 2:** A 55-year-old male presented with vertebrogenic low back pain of 2 years duration. (A, B & C): Sagittal T1-weighted MR image, sagittal T2WI, Sagittal STIR MR image of lumbar spine. Show (A) hypo-intensity, (B) hyperintensity signal, (C) hyperintensity signal at the involved bone marrow of both vertebral bodies at the (L2-3) level. (D, E& F): Sagittal diffusion-weighted MR image of lumbar spine with different b values: (D) b-value of 50 s/mm². (E) b-value of 500 s/mm². (F) b-value of 800 s/mm², the red arrows indicate the lesion at the vertebral endplate, demonstrating the claw

sign across different sequences." The claw sign is a well-defined, curvilinear hyperintensity at the junction between normal and abnormal marrow signals in the vertebral endplates on DWI, forming a "claw-like" pattern that is decreasing with increasing b-value. (G) sagittal lumbar DWI at b value 800 s/mm<sup>2</sup>&(H) corresponding sagittal lumbar ADC map. The lesion shows restricted diffusion (high signal at DWI, low at ADC map). The ROI on the lesion yields an ADC value of 1.325 × 10 <sup>-3</sup> mm<sup>2</sup>/s. This case was confirmed to have MODIC I degenerative changes by follow-up.

Bessar, et al 5370 | Page

#### **DISCUSSION**

In line with earlier reports, the observed signal pattern of T1 hypointensity with T2 hyperintensity was found in both infectious spondylitis and Modic type I changes, which explains the diagnostic uncertainty at early stages. In our series, conventional MRI reached an overall accuracy of 84.8%, with a sensitivity of 87.5% and specificity of 77.8%, reflecting its limitations for precise differentiation. This underscores the added value of functional imaging such as DWI and ADC mapping, which can provide microstructural insight beyond morphology [12,13].

In our study, mean ADC values were lower in infection  $(0.97 \times 10^{-3} \text{ mm}^2/\text{s})$  in early  $\times 10^{-3}$ changes, 0.80 mm²/s in spondylodiscitis) compared with Modic I degeneration  $(1.29 \times 10^{-3} \text{ mm}^2/\text{s})$ , reflecting restricted diffusion from cellularity and pus. Our results are consistent with those of Dagestad MH et al. [12] and Choi SH et al.[13], who observed that in Modic type I changes, increased extracellular water from marrow depletion results in higher ADC values and low signal intensity on DW images, while acute infectious spondylitis demonstrates reduced extracellular volume from infiltration, inflammatory cell producing low ADC values and high DW signal.

Similarly, prior studies reported mean / median ADC values in infectious spondylitis ranging between  $0.79-1.16 \times 10^{-3}$  mm<sup>2</sup>/s, which aligns closely with the present findings  $(0.81-1.05 \times 10^{-3}$  mm<sup>2</sup>/s) as shown by Daghighi et al. [14] and Crombé et al. [7].

By contrast, Eguchi et al. [15] documented lower mean ADC values in Modic changes  $(0.62 \pm 0.32 \times 10^{-3} \text{ mm}^2/\text{s})$  compared with infection  $(1.07 \pm 0.12 \times 10^{-3} \text{ mm}^2/\text{s})$ , which differs from our observations. It is important to note that higher ADC values generally represent increased water mobility in the

sampled ROI, whereas lower values reflect restricted diffusion due to reduced extracellular space [16].

This discrepancy with Eguchi et al. [15] may be partly explained by differences in disease stage and treatment status. When infection is subacute or therapy has already been initiated, ADC values may decline compared to acute untreated cases due to reduced inflammatory activity and regression of edema. This phenomenon was emphasized by Boruah et al. [17], who noted that in treatment responders, there was a greater drop in ADC values after therapy.

In our study, an ADC cutoff value of >1.19  $\times 10^{-3}$ mm²/s demonstrated superior diagnostic performance compared with conventional differentiating MRI for infectious spondylitis from Modic type I degeneration, particularly in terms of specificity and positive predictive value. suggests that a positive This **ADC** measurement provides high reliability for confirming infection, reducing false-positive diagnoses, and offering strong diagnostic confidence. However, the relatively lower sensitivity and negative predictive value highlight that ADC quantification is best used as a confirmatory tool in cases where conventional MRI findings remain inconclusive.

Comparable outcomes have been documented previously. Daghighi et al. [18] identified an optimal ADC cutoff of 1.52  $\times 10^{-3}$ mm<sup>2</sup>/s, which achieved excellent specificity (100%) and sensitivity (91.7%) differentiating infection for from degenerative marrow changes. Similarly, Boudabbous S et al. [19] reported mean ADC values of  $1.27 \pm 0.38 \times 10^{-3}$  mm<sup>2</sup>/s in infectious spondylodiscitis, supporting the utility of ADC as a reliable discriminator in this clinical context.

The use of both qualitative DWI signs and quantitative ADC thresholds provides a dual-layered diagnostic approach. This

**Bessar**, et al **5371** | P a g e

multiparametric strategy improves specificity, minimizes false positives, and enhances overall diagnostic accuracy in challenging cases.

Among qualitative signs, the "claw sign" has been well described. Tanenbaum et al. [20] reported that restricted diffusion at the advancing boundary of Modic type I lesions produces a sharp, well-defined hyperintense "claw" on DW images. Its presence is highly consistent with degenerative disease and demonstrates very high predictive value. amorphous, ill-defined Conversely, an hyperintensity pattern has been suggested as a strong indicator of osteomyelitis and infection, also emphasized by Crombé et al. [7].

study, the claw In our sign also diagnostic demonstrated perfect performance, with sensitivity, specificity, PPV, NPV, and accuracy all reaching 100% for distinguishing Modic type I changes from infectious spondylitis. Conversely, the amorphous increased signal pattern showed very good diagnostic reliability, with a sensitivity of 96.4%, a specificity of 95.8%, a PPV of 96.1%, an NPV of 95.7%, and an overall accuracy of 96.0%. These findings further validate the robustness of the claw sign for confirming Modic I degeneration and the utility of an amorphous increased signal in identifying infection.

In this study, DWI was assessed at bvalues of 50, 500, and 800 s/mm<sup>2</sup>. Both Modic I and infectious lesions appeared hyperintense at b=50 s/mm<sup>2</sup>, but differences became clearer with higher gradients. At b =800 s/mm<sup>2</sup>, hyperintensity persisted in only 5.6% of Modic I cases versus 85.7% of infections (p < 0.001). This highlights the value of high b-value DWI in detecting restricted diffusion from pus inflammatory infiltration. These results align with Daghighi et al. [18], who reported the claw sign in Modic I (especially at b = 50 s/mm²) but not in infection. while

amorphous signals appeared only in infection. Both signs showed 100% diagnostic accuracy in differentiating Modic I from spondylitis.

Our findings agree with Daghighi et al. [18], who showed that high b-value imaging (800 s/mm²) improves specificity by reducing T2 shine-through. In our work, b = 800 s/mm<sup>2</sup> yielded 94.4% specificity and 92% accuracy, close to their reported 96.8% and 95.3%. Few studies have directly compared Modic type I changes with infection. Geith et al. [21] ( $b = 500 \text{ s/mm}^2$ ) observed hyperintense signals in all acute spondylodiscitis cases, while Zhang et al. [22] (b =  $1000 \text{ s/mm}^2$ ) noted persistent hyperintensity in infection but iso-/hypointensity in Modic type I. Kapoor et al. [23] emphasized that selecting the optimal b-value is crucial for balancing diffusion signal-to-noise in lesion weighting and characterization.

Our results align with Lakouz et al., who reported that DWI and ADC measurements help differentiate early infectious spondylodiscitis from Modic type I changes, with infectious lesions showing lower ADC values and Modic changes demonstrating higher values [24].

Our data also demonstrated that benign fractures typically lack true diffusion restriction, exhibiting intermediate-to-low signals on high b-value images and high ADC values, reflecting edema rather than cellular infiltration, which aids in differentiating them from infection even without a trauma history. This functional imaging distinction enabled confident differentiation of benign fractures from infection, particularly in cases without an obvious history of trauma. These findings are consistent with Balliu et al. [25], who reported ADC values of approximately 1.9  $\times 10^{-3}$  mm<sup>2</sup>/s in acute benign vertebral collapse compared with  $0.96 \times 10^{-3}$  mm<sup>2</sup>/s in infectious spondylitis. In our series, acute

**5372** | P a g e

benign fractures showed higher ADC values  $(1.67 \pm 0.19)$ , while infectious spondylodiscitis remained significantly lower  $(0.93 \pm 0.12)$ .

Previous studies shown have that osteoporotic fractures exhibit higher ADC values than malignant fractures due to marrow edema and trabecular disruption, which increase water diffusivity. Qualitative DWI features also aid diagnosis, with usually malignant lesions appearing hyperintense and osteoporotic ones iso- to hypointense. Dietrich et al. [26] highlighted the importance of combining **ADC** thresholds with visual assessment for accurate differentiation.

Vertebral hemangiomas, though often incidental, may mimic aggressive lesions in atypical forms. In our series. typical hemangiomas showed no diffusion restriction, low-to-intermediate DWI signal at high b-values, and elevated ADC values (mean:  $1.35 \times 10^{-3} \text{ mm}^2/\text{s}$ ), reflecting their vascular nature. Even atypical hemangiomas exhibited intermediate-to-high ADC values  $(0.80 \pm 0.57 \times 10^{-3} \text{ mm}^2/\text{s})$ , supporting their benign histology.

Degenerative Modic subtypes also revealed distinct diffusion profiles. Modic II changes showed no restriction, low DWI signal, and high ADC values (mean:  $1.46 \times 10^{-3}$  mm<sup>2</sup>/s), consistent with fatty marrow replacement, whereas Modic III changes had lower ADC values (mean:  $0.55 \times 10^{-3}$  mm<sup>2</sup>/s) due to sclerosis, but showed no diffusion their chronic, restriction, highlighting and excluding inactive nature malignant infiltration.

These findings are in agreement with a recent large-scale meta-analysis summarized by Dietrich et al. [26], which demonstrated that benign vertebral bone marrow lesions consistently show higher ADC values (mean  $\sim 1679 \pm 531 \times 10^{-6}$  mm²/s) compared with malignant lesions (mean  $\sim 913 \pm 354 \times 10^{-6}$  mm²/s), independent of b-value selection or

magnet field strength. This meta-analytic evidence supports the clinical validity of our results, strengthening the role of ADC quantification in vertebral lesion characterization.

In the present study, a significant difference was found in mean ADC values between the cases  $(1.10 \pm 0.47)$  and the control group  $(0.26 \pm 0.08)$  (p<0.001), reinforcing that vertebral pathologies exhibit diffusion compared altered to normal The control group exhibited marrow. facilitated diffusion and normal vertebral body signals, establishing a reliable imaging Yet nearly 73% had baseline. some abnormalities (disc bulge, back muscle spasm), despite being classified as controls. This highlights the nonspecificity of back pain symptoms and the importance of correlating imaging findings with the clinical context. In terms of associated symptoms, LL paraesthesia and numbness were more common in the control group; these symptom profiles may aid in clinical although symptom overlap stratification, limits their standard of utility.

Strengths of this study include using both qualitative DWI and quantitative ADC analysis with multiple b-values, enhancing diagnostic accuracy, and including a control group for baseline comparison.

**Limitations:** The study is limited by its single-center design and relatively small sample size. Histopathological confirmation was not consistently available, and prior treatments may have influenced ADC values. These factors should be considered when interpreting the findings.

Recommendations: We recommend future studies with larger, multi-center cohorts to validate ADC thresholds, comparative analyses of DWI versus contrast-enhanced MRI in equivocal cases, and inclusion of additional benign and malignant spinal pathologies to enhance clinical applicability.

**5373** | P a g e

#### **CONCLUSION**

Diffusion-weighted imaging and apparent diffusion coefficient mapping significantly improve the differentiation of infectious spondylodiscitis from Modic type I changes, with high b-value DWI (800 s/mm²) and ADC thresholds offering superior accuracy. The claw sign and amorphous hyperintensity further aid early distinction at lower b-values

In addition, DWI and ADC provided useful functional insights for other benign spinal conditions, complementing conventional MRI. Incorporating these techniques into routine practice enhances diagnostic confidence, reduces false positives, and supports more precise patient management.

Conflict of Interest & Funding Statement: This work was completed independently, with no external funding, and the authors report no competing interests.

**Data Availability:** Requests for access to the underlying data that substantiate the results of this study may be directed to the corresponding author, who will consider providing them in accordance with institutional policies and applicable ethical guidelines.

**Author contribution:** A.A.B. and K.M.S. were instrumental in shaping the research methodology, providing hypothesis and expert guidance throughout the project's development. R.M.A.E.R.H. contributed to imaging protocol, data interpretation, and analytical validation. M.N.M.A., capacity as a resident in the department and the corresponding author, was primarily responsible for conducting the clinical data collection, managing case selection, and manuscript. drafting the She also coordinated all revisions and communication with co-authors. All contributors reviewed and approved the final manuscript before submission.

**Supplementary material:** Table 1S, Figure 1S, 2S

#### REFERENCES

- GBD 2021 Low Back Pain Collaborators. Global, regional, and national burden of low back pain, 1990–2020, its attributable risk factors, and projections to 2050: a systematic analysis of the Global Burden of Disease Study 2021. Lancet Rheumatol. 2023;5(6):e316–29.
- Zhang J, Bellow E, Bae J, Johnson D, Bajrami S, Torpey A, et al. Modic changes as biomarkers for treatment of chronic low back pain. Biomedicines. 2025;13(7):1697.
- 3. Mahendram S, Christo PJ. Advances in basivertebral nerve ablation for chronic low back pain: a narrative review. J Pers Med. 2025;15(3):119.
- 4. Cao Z, Zhang M, Jia J, Zhang G, Li L, Yang Z, et al. Incidence and risk factors for Modic changes in the lumbar spine: a systematic review and meta-analysis. Front Endocrinol. 2025;16:1585552.
- Yang D, Hoehl BU, Schönnagel L, Mödl L, Zhang T, Liu S, et al. Modic changes are associated with increased pain intensity, greater disability, and reduced quality of life in low back pain: a crosssectional study. Clin Orthop Relat Res. 2022;Epub ahead of print.
- Schnapp W, Schnapp M, Gottlieb J, Alexandre LC, Martiatu K, Delcroix GJR. Prospective cohort study of basivertebral nerve ablation for chronic low back pain in a real-world setting: 12 months follow-up. Interv Pain Med. 2024;3(4):100446.
- Crombé A, Fadli D, Clinca R, Reverchon G, Cevolani L, Girolami M, et al. Imaging of spondylodiscitis: a comprehensive updated review multimodality imaging findings, differential diagnosis, and specific microorganisms detection. Microorganisms. 2024;12(5):893.
- 8. Zhang C, Liu S. The advancement of MRI in differentiating Modic type I degenerative changes from early spinal infections. Br J Radiol. 2023;96(1152):20230551.
- Alghadir A, Anwer S, Iqbal ZA, Alsanawi HA. Cross cultural adaptation, reliability and validity of the Arabic version of the reduced Western Ontario and McMaster Universities Osteoarthritis Index (ArWOMAC) in patients with knee osteoarthritis. Disabil Rehabil. 2016;38(7):689–94.
- Kim Y, Lee YJ, Lee Y, Park HJ, Choi SH, Moon JH. Pitfalls of diffusion-weighted imaging: clinical utility of T2 shine-through effect and apparent diffusion coefficient mapping. Diagnostics (Basel). 2023;13(9):1647.
- 11. Boudabbous S, Gangi A, Dap F, et al. Spinal disorders mimicking infection: imaging features and

**5374** | Page

- diagnostic pitfalls. Insights Imaging. 2021;12(1):1–12.
- Dagestad MH, Vetti N, Kristoffersen PM, Zwart JA, Storheim K, Bakland G, et al. Apparent diffusion coefficient values in Modic changes – interobserver reproducibility and relation to Modic type. BMC Musculoskelet Disord. 2022;23:695.
- 13. Choi SH, Hwang JM, Lee S, Lee SY, Jung JY. Diagnosis of infectious spondylitis using non-contrast enhanced MRI with axial diffusion-weighted images: comparison with gadolinium-enhanced MRI. Investig Magn Reson Imaging. 2023;27(2):75–83.
- 14. Daghighi MH, Rehman S, Laufer L, Sharma R, Idrees S, Sendhi D, et al. The role of b-value, apparent diffusion coefficient, claw sign, and chemical shift in differentiating acute infectious spondylitis from Modic type 1 change. Eur Radiol. 2016;26(10):3510–21.
- 15. Eguchi Y, Ohtori S, Yamashita M, Yamauchi K, Suzuki M, Orita S, et al. Diffusion magnetic resonance imaging to differentiate degenerative from infectious endplate abnormalities in the lumbar spine. Spine. 2011;36(3):E198–202.
- 16. Fliedner FP, Engel TB, El-Ali HH, Hansen AE, Kjaer A. Diffusion-weighted magnetic resonance imaging (DW-MRI) as a non-invasive, tissue cellularity marker to monitor cancer treatment response. BMC Cancer. 2020;20(1):134.
- 17. Boruah DK, Majumder D, Choudhury A, Sarma D, Borgohain S. Added advantages of DWI MR imaging and ADC mapping: changes in ADC values in treatment responders in vertebral infection. J Clin Imaging Sci. 2025;15:42.
- 18. Daghighi MH, Poureisa M, Safarpour M, Behzadmehr R, Fouladi DF, Meshkini A, et al. Diffusion-weighted magnetic resonance imaging in differentiating acute infectious spondylitis from degenerative Modic type 1 change: the role of bvalue, apparent diffusion coefficient, claw sign and

- amorphous increased signal. *Br J Radiol*. 2016;89(1066):20150152. doi:10.1259/bjr.20150152.
- 19. Boudabbous S, Luraschi A, Gauthier A, Meli DN, Becker CD, Ratib O, et al. Differentiating infectious spondylodiscitis from degenerative Modic type 1 changes using diffusion-weighted imaging and apparent diffusion coefficient mapping: preliminary results. Insights Imaging. 2021;12(1):138.
- 20. Tanenbaum LN. Diffusion imaging in the spine. Appl Radiol. 2011;40(4):9-15.
- 21. Geith T, Baur A, Schick F, et al. Comparison of qualitative and quantitative evaluation of diffusion-weighted MRI and chemical-shift imaging in the differentiation of benign and malignant vertebral body fractures. AJR Am J Roentgenol. 2012;199(6):W687–93.
- 22. Zhang Y, Li Y, Zhang Y, et al. Diffusion-weighted magnetic resonance imaging and apparent diffusion coefficient mapping for diagnosing infectious spondylodiscitis: a preliminary study. J Neuroimaging. 2014;24(4):383–8.
- 23. Kapoor R, Kapoor A, Kapoor S, et al. Apparent diffusion coefficient and T2\* mapping on 3T MRI in normal and degenerative lumbar intervertebral discs: a comparative study. Pol J Radiol. 2023;88:e163021.
- 24. Lakouz K, Radwan H, Sarhan A, Elmolla R. Role of diffusion-weighted magnetic resonance imaging in characterization of vertebral bone marrow pathological lesions. Zagazig Univ Med J. 2013;19(6):1–12.
- 25. Balliu E, Vilanova JC, Peláez I, Puig J, Remollo S, Barceló C, et al. Diagnostic value of apparent diffusion coefficients to differentiate benign from malignant vertebral bone marrow lesions. Eur J Radiol. 2009;69(3):560–6.
- 26. Dietrich O, Geith T, Reiser MF, Baur-Melnyk A. Diffusion imaging of the vertebral bone marrow. NMRBiomed.2017;30(3):e3333

### Supplementary material:

**Table 1S:** Conventional MRI Signal Intensities, Associated Findings in Cases, and Imaging Features in Controls

MRI Feature	Cases Group (n = 48)	Controls Group (n = 48)
Vertebral Lesion Signal		
Intensities		
T1WI Iso-intense	1 (2.1%)	_
T1WI Hypo-intense	40 (83.3%)	_
T1WI Hyper-intense	7 (14.6%)	_
T2WI Iso-intense	0 (0.0%)	_
T2WI Hypo-intense	5 (10.4%)	_
T2WI Hyper-intense	43 (89.6%)	_
MRI-Associated Findings		
(Cases only)		

**Bessar**, et al **5375** | Page

MRI Feature	Cases Group (n = 48)	Controls Group (n = 48)
Loss of lumbar lordosis	30 (62.5%)	_
Spondylolisthesis	5 (10.4%)	_
Disc bulge / herniation	18 (37.5%)	_
Soft tissue thickening	2 (4.2%)	_
Ligamentum flavum	5 (10.4%)	_
hypertrophy		
Overall Imaging Features	_	Normal signal of the lumbar
(Controls)		vertebrae on conventional MRI;
		Facilitated diffusion in
		vertebral bodies on DWI

MRI: Magnetic Resonance Imaging; T1WI: T1-weighted imaging; T2WI: T2-weighted imaging; DWI: Diffusion Weighted Imaging.

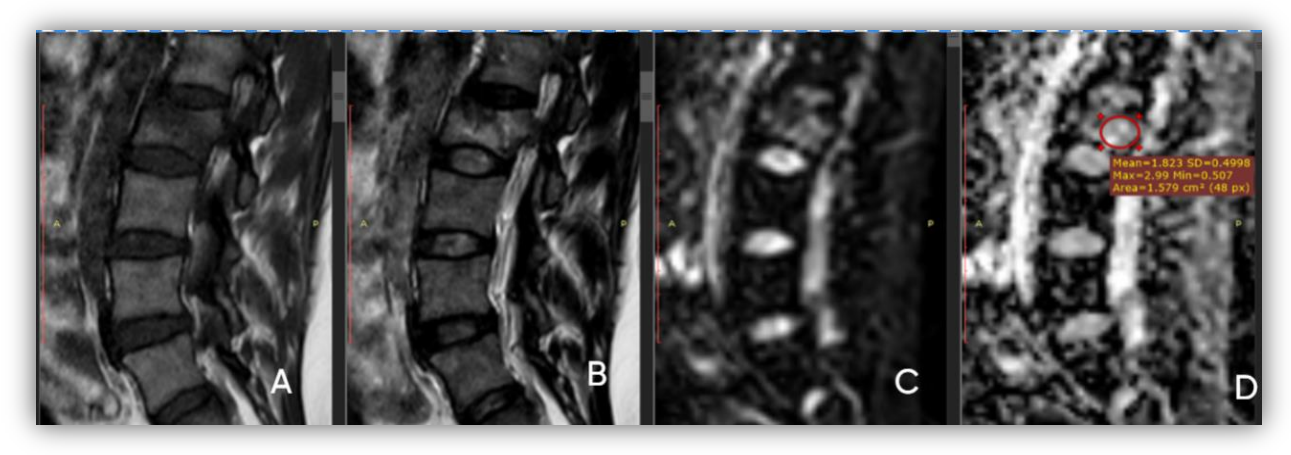




**Figure 1S:** A 30-year-old female presented with vertebrogenic low back pain (**A**, **B**, **C**, **D** &E). (**A**) Sagittal T1-weighted image of lumbar spine showing a hypointense lesion of the L2 vertebral body. (**B**) Sagittal T2-weighted image of lumbar spine showing a hyperintense lesion of the L2 vertebral body. (**C**) Sagittal lumbar DWI at (b value 800 s/mm<sup>2</sup>): The vertebral body lesion shows an

isointense signal. **(D)** Corresponding ADC map: The lesion shows high signal, matching facilitated diffusion. ROI on the lesion (ADC value: 1.823 x **10** <sup>-3</sup> mm<sup>2</sup>/sec). the case was confirmed to have an L2 compression fracture by CT (**E**). Sagittal lumbar spine CT shows a compression fracture of the L2 vertebrae.

Bessar, et al 5376 | Page



Figure 2S: WOMAC score [9]

#### Citation

Bessar, A., Shawky, K., Attia, M., Hassan, R. Using A Quantitative Assessment Tool in Diffusion Weighted Magnetic Resonance Imaging in Patients with Non-Neoplastic Vertebrogenic Low Back Pain. *Zagazig University Medical Journal*, 2025; (5362-5377): -. doi: 10.21608/zumj.2025.419825.4147

Bessar, et al 5377 | Page